## Model-Based Control Design for a Multi-Stacks SOC System

Axelle Hégo<sup>1</sup> Félix Bosio<sup>1</sup> Sylvain Mathonnière<sup>1</sup>

<sup>1</sup>Univ. Grenoble Alpes, CEA/LITEN, 17 Rue des Martyrs, 38054 Grenoble Cedes 9, France, {axelle.hego, felix.bosio, sylvain.mathonniere}@cea.fr

#### **Abstract**

In response to growing interest in high-temperature electrolysis, CEA-Liten has developed multi-stack Solid Oxide Cell (SOC) testing equipment comprising four electrolyser stacks. Each stack includes multiple cells, and together they form a module housed within a shared thermal enclosure and connected to a balance of plant. This setup supports the development of innovative control strategies, essential due to the stacks' sensitivity to operating conditions. To mitigate risks and costs associated with testing new strategies directly on the physical system, a Model in the Loop approach was implemented. The model replicates the real module's characteristics and operational capabilities, allowing safe and efficient design and validation of control strategies. Various transition scenarios between operating conditions—tailored to diverse production needs and constraints—were developed and validated using the model before real-world implementation. This paper presents the model-based control methodology and compares experimental results with simulations.

Keywords: system modeling, FMU, control design, Solid Oxide Electrolysis Cell SOEC

### Acronyms

BoP Balance of Plant.

FMI Functional Mock-up Interface.

FMU Functional Mock-up Unit.

**HEX** Heat EXchanger.

**HTE** High Temperature Electrolysis.

MiL Model in the Loop.

PFD Process Flow Diagram.

PLC Programmable Logic Controller.

**SC** Steam Conversion.

**SOC** Solid Oxide Cell.

**SOEL** Solid Oxide Electrolyser.

#### 1 Introduction

Hydrogen  $(H_2)$  production based on water electrolysis can contribute significantly to the decarbonisation objectives of the energy and industry sectors. High Temperature Electrolysis (HTE) based on Solid Oxide Cell (SOC) technology is currently in industrialisation phase with the start of MW scale demonstrators (Iyer et al. 2024). Solid Oxide Electrolyser (SOEL) systems are composed of modules containing several stacks in the same thermal enclosure and supplied by the Balance of Plant (BoP) with

gases at the required conditions (composition, temperature, pressure) and with electrical current. In this context, CEA-Liten has developed a highly instrumented four stacks module presented in (Cubizolles et al. 2024). The operation of such modules is complex due to high sensitivity for some operating parameters, such as pressure or current. It is also time-consuming and cost-expensive in terms of human resources and equipment. Using multiphysic modelling is interesting to investigate behavior of the system and test new control strategies without risking to damage the real components. Once validated on the model, the new control strategies can be implemented in the real Programmable Logic Controller (PLC) and validated on the real module.

System modelling has two broad applications: design and sizing at the early phase of a project and model-based control development (Iver et al. 2024). For this second application, the Model in the Loop (MiL) methodology is used. This methodology aims at developing low (PID) to high-level (Model Predictive Control (MPC)) control laws by leveraging the modelling of actuators and using return states of the modelled system as input to the control models (Aoun et al. 2019). Extensions of this methodology are Software in the Loop (SiL) where the algorithm control itself is compiled and tested with a simulated model and then Hardware in the Loop (HiL) in which the hardware itself (controller hardware in this case) is included, most of the time requiring real-time simulations (Zimmer 2019). This paper presents a MiL methodology based on a plant modelling using Modelica language, an export of this model as a Functional Mockup Unit (FMU) (Modelica Association 2014) and then a co-simulation in Simulink (The MathWorks Inc. 2025a) where the control development has been implemented. This workflow can be used on almost all types of system such as in (Cech et al. 2017) with a steam turbine model, (Wang et al. 2017) with a model of refrigerant system for vehicle, and (Ensbury, Horn, and Dempsey 2020) with a vehicule model. Concerning model-based control for SOC, most studies are focuses on the coupling with other systems (nuclear, solar, etc) (Iyer et al. 2024). To the authors' knowledge, few studies have investigated specific control. In (Botta et al. 2019), SOFC and SOEC 1D dynamic stacks are modelled using Modelica and then PI controllers are defined to manage temperature of these two modes. In (Pohjoranta et al. 2015), MPC

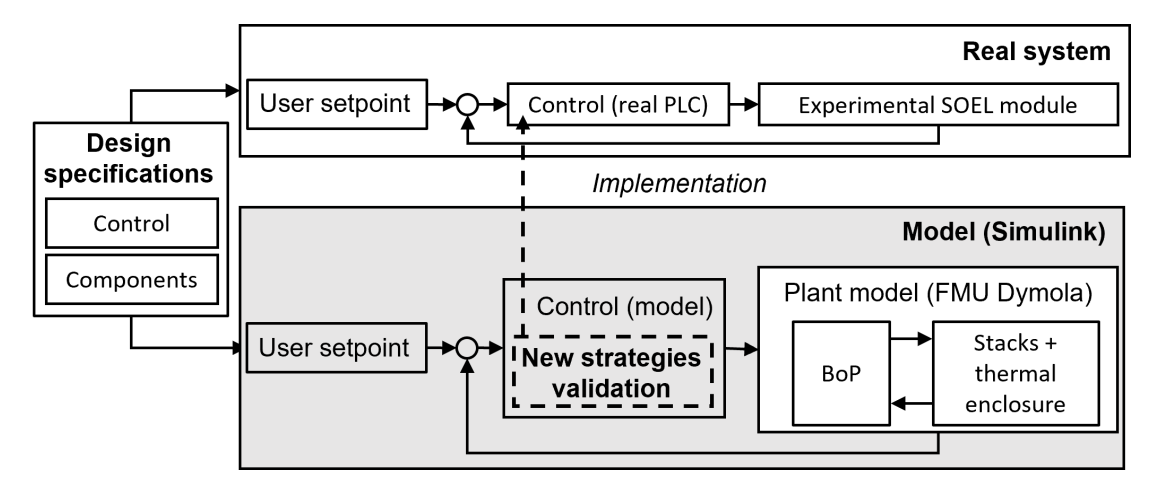


Figure 1. Overview of model-based design for control applied on a SOEL module

approach is applied on SOFC stack temperature based on experimental data of a SOFC system. In the present work, control strategies to change operating conditions are applied on a complete one-module system model and its real system counterpart. These strategies involve stacks' temperatures, gases flow rates (thus composition), current and voltage regulation.

This paper describes the methodology applied to the multi-stacks one-module system of the CEA-Liten by presenting a global model overview in Section 2. The represented system is briefly described as well as the corresponding Dymola model. The control model and control strategies are also presented. Illustration of high-level control strategies are presented in Section 3 towards a comparison between experimental and simulated data. Section 4 concludes with perspectives and challenges of the study.

## 2 Model and methodology

#### 2.1 Model overview

This study focuses on a model of the multi-stacks testing equipment presented in (Cubizolles et al. 2024). A complete system model is developed using different software tools as shown in Figure 1. The Modelica language is tailored to represent complex multi-physics dynamics whereas the Simulink software is ubiquitous for control development, therefore they were selected for the development of respectively the plant model and the control model. The Functional Mock-up Interface (FMI) standard is well suited for encapsulating systems of ordinary differential equations and more generally for Modelica models, therefore in order to exchange data between those two models, the plant model was encapsulated in a Functional Mock-up Unit (FMU) based on this standard to be co-simulated in Simulink software along with the control model.

The FMU of the plant model comprises about 30 inputs which correspond to the actuator commands provided by a control model. The FMU outputs are about 90 and represent state returns representing simulated sensors which describe model system behavior. All the components of this complete system model are configured using real system specifications such as datasheet of components, measured quantities and control loop implemented in real PLC.

#### 2.2 Plant model on Dymola

The dynamic plant model is composed of three interconnected subsystems: fuel loop, air loop and hotbox. The BoP refers to the fuel loop and the air loop which supply the conditioned fluids to the hotbox subsystem. The hotbox comprises four stacks designed and manufactured by CEA (individual power of 2.5  $kW_{DC}$ ), heaters, Heat EXchanger (HEX) and the thermal enclosure (hotbox) in which they are contained. Figure 2 is a simplified Process Flow Diagram (PFD) of the electrolysis configuration of the system.

- The **fuel loop** corresponds to the steam and hydrogen conditioning upstream of the hotbox and downstream until venting. The HEXs in series (Figure 2 (A) and (B)) heat the inlet fuel using heat from fuel downstream from the stacks. The heater (C) is controlled to supply hotbox subsystem with fuel at required temperature. The unconverted steam/ $H_2$  mix in the reactant line downstream from the stacks and HEX is condensed in (E) before venting.
- The **air loop** is fed by the blower (Figure 2 (b)) and a by-pass ensures the flow rate. Upstream from the blower, a HEX (a) removes excess humidity from the air with water cooling. Then, inlet air is heated up by HEX (c) using heat from air downstream from the stacks and the heater (d) before the hotbox. As

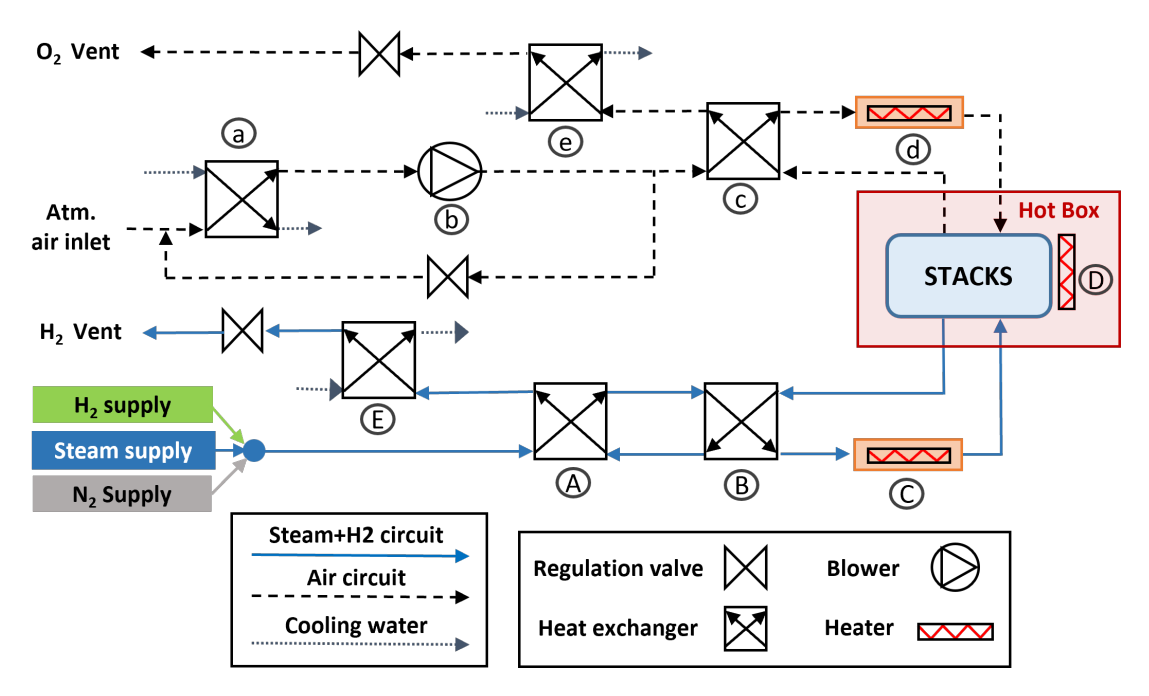


Figure 2. Process flow diagram of SOEL system from (Cubizolles et al. 2024)

with fuel, air downstream from stacks and HEX is cooled down before vent.

- Gas feeding of the loops are represented with gas sources of fixed pressures (Modelon Pressure boundary components) where media of Fuel Cell library media are used. Fuel media corresponds to "PreDefined.IdealGases.FastSteamHydrogen" composed of  $H_2O$ ,  $H_2$  and  $N_2$ . Air media corresponds to "PreDefined.IdealGases.FastMoistAir" composed of  $H_2O$ ,  $N_2$  and  $O_2$ .
- In the hotbox subsystem, fluids (air & reactant) flow through HEXs that connect the upstream and downstream flows from stacks for each medium. Then, the air and reactant are distributed respectively at the anode and cathode of the four stacks. The four stacks are positioned in a 2×2 vertical grid in a thermal enclosure comprising three heaters (Figure 2 (D)). In order to model the hotbox subsystem, the four stacks are represented by a vector of stack model based on SOFC stack component of a commercial Fuel Cell Library (Andersson et al. 2011) and connected fluidically and electrically in parallel. The stack model is composed of two reaction pipes (anode and cathode) which exchange mass and heat information with a electrochemical model. It corresponds to a reduced model based on experimental data and a CEA's Single Repeat Unit (SRU) model (Laurencin et al. 2011). Stacks' temperatures are computed through four thermal models (one per stack) taking into account conductive heat transfer, and, through a source term added to the heat equation, heat generated by electrochemical reaction and the gases enthalphy dif-

ference. The thermal model of the hotbox is composed of a network of thermal capacities representing stacks environment (heaters, stacks' supports) and the walls (~130 heat capacitors) without the stacks themselves. The four stacks included in the hotbox are each represented with 41 continuous state variables that are used to perform a thermal mapping of the stack. The stacks environment, its interactions with the stacks and interactions between stacks are computed with the network of heat capacitors linked by conductive and radiative transfers. Those heat transfer models are all finely tuned through external 3D Computational Fluid Dynamic (CFD) simulations.

Plant model had been implemented using Dymola software v2023x Refresh 1 (Dassault Systèmes 2025) as integrated development environment for Modelica Standard Library (MSLv3.2.3) and Modelon (MBLv3.7) - Fuel Cell Library (FCLv1.13) (Modelon AB 2021a; Modelon AB 2021b). The model is composed of:

- valves<sup>1</sup> with a quasi-static isenthalpic flow neglecting mass and energy storage, based on IEC 534/ISA S.75 standards for valve sizing.
- semi-empirical compressor models<sup>2</sup>, implementing polytropic processes and quasi-static substance mass and energy balances are used. Both centrifugal and reciprocating compressors models have been chosen to best fit the experimental hardware.
- heat exchangers, for heat recovery from stack downstream fluid (Fig. 2 (A), (B) and (C)), represented

<sup>&</sup>lt;sup>1</sup>Modelon.ThermoFluid.Valves.ValveCompressible

<sup>&</sup>lt;sup>2</sup>Modelon.ThermoFluid.Compressors.DynamicCompressor and PositiveDisplacementCompressor

- with dynamic NTU lumped exchanger using Modelon convective heat transfer model<sup>3</sup> and effectiveness functions<sup>4</sup> or value adapted to real components.
- heat exchangers<sup>5</sup>, for cooling (Fig. 2 (a), (e) and (E)), represented with lumped model of indirect cooler using the logarithmic mean temperature difference for heat transfer calculation.
- friction models represented with static isenthalpic flow incorporating lumped pressure loss without energy or mass storage.

Valve parameters (opening flow characteristics and flow coefficient), compressor parameters (efficiency and flow maps) are set using components' data sheet and, in some models, based on experimental data.

The complete model once translated contains about 500 continuous time states. The hotbox thermal model dynamic being of paramount interest for HTE, it contains more than 300 continuous time states. The remaining states are distributed between the thermofluidic states of the fluids (~60 for the air loop, ~70 for the fuel loop and ~30 for the hotbox) and the stacks' electrochemistry.

This plant model has been encapsulated in FMU, v2.0, in co-simulation using implicit solver (Radau) which is stable for stiff thermofluidic models with a tolerance of 1e-4.

#### 2.3 Control model on Simulink

The control of complex systems can be organized in two main parts:

- The low-level control corresponds to the signals applied directly to actuators. These signals could come from direct inputs (an opening value for a valve for example) or from set-point drived controllers, like the PID ones. This type of controllers compares a measured signal to a set-point and computes a correction signal to send to the actuator which impacts the measured variable.
- The high-level control corresponds to set-points definition. It can be as basic as direct values or more elaborate, with user-defined functions describing the logic to take into account, using a set of parameters, inputs, limitations, laws, etc.

For SOEL systems, the main goal is to produce a certain amount of  $H_2$ . To do this, the main variables to control are:

- the gases flow rates,
- the gases composition,

- the current density,
- the stacks' temperature.

In addition, other important variables need to be monitored in order to take into account the stacks limitations or users' requirements. Some are from direct measurements, as the cells voltage U, others are build from other variables. From this last category, the Steam Conversion (SC) is one of the most important and is defined as:

$$SC = \frac{j}{2F} * \frac{1}{\dot{n}_{H_2O}} \tag{1}$$

with the current j in A, F the Faraday's constant  $(96485 A \cdot s \cdot mol^{-1})$  and the molar flow rate of inlet steam  $\dot{n}_{H_2O}$  in  $mol \cdot s^{-1}$ .

The nominal way of controlling the considered system for a constant  $H_2$  production demand is to have the current density and the SC to the highest safe values possible. With these parameters fixed, Equation 1 leads to the flow rates values calculation. Then, the last parameter to determine is the stacks' operating temperature. In the current framework, it is controlled by the stacks' mean voltage value. The voltage target is the thermoneutral voltage (~1.287 V for one cell) where heat sources generated by the electrochemical process irreversibilities (such as omhic losses) are counterbalanced by the endothermicity of the electrolysis reaction. For a given flow rate and current density, only one temperature leads to operating the stacks at their thermoneutral mean voltage. The aim is to maintain the stacks voltage close to this value during their lifetime, by adjusting the temperature to compensate the voltage increase due to degradation phenomena.

It is expected that SOEL systems are operated in stationary mode, some punctual modulation of the production rate can be required. It could come from the final  $H_2$  consumer or from inputs limitation as the electricity or steam availability.

Different strategies can be imagined to adapt the production rate of the system but they will all lead to modifications of the main parameters set-points (flow rates, current density and stacks' temperature). The way of applying these modifications can be critical for the stacks integrity and can cause irreversible damages. In order to limit the risks taken on the real system, the model-based control design approach is a pertinent solution for the test, the comparison and the validation of these strategies.

This study focuses on the comparison of two different strategies for an operating point transition:

 The slow transition, described by the state transition control diagram in Figure 3, aim to modulate the H<sub>2</sub> production with a constant SC. The first step

<sup>&</sup>lt;sup>3</sup>Modelon.ThermoFluid.Volumes.HeatTransfer.LumpedHT\_Dittus-Boelter and LumpedHT\_constAlpha

<sup>&</sup>lt;sup>4</sup>Modelon.ThermoFluid.HeatExchangers.Functions.parallelFlow and counterFlowEps

<sup>&</sup>lt;sup>5</sup>FuelCell.HeatExchangers.GasWater.GasDryer

is to start a ramp on the temperature (T ramp) to a higher or lower set-point (respectively for more or less  $H_2$  production). The temperature evolution impacts the stacks' voltage value U and the current j can be increased or decreased by  $\Delta j$  to stay at the thermoneutral voltage  $U_{THN}$ . The current evolution would modify the SC value so the steam flow rate is adjusted to keep it constant. The last step corresponds to the stop of the temperature ramp. It is reached when the current is at its target value.

• The fast transition, as outlined in the state transition control diagram in Figure 4, enables the SC to adjust quickly by evolving the flow rate in order to reach the new current set-point as quickly as possible, while keeping the stacks at the thermoneutral voltage. To achieve this, a flow rate ramp (Q ramp) is initiated simultaneously with the temperature ramp (T ramp). It leads to a faster evolution of the voltage, compared to the temperature ramp only in the slow transition, that can be compensated by current variations. Once the new current set-point is reached, the flow rate ramp is halted, and the SC is gradually returned to its initial value by incrementing the flow rate, as the temperature change influences the voltage.

The described control model is based on the same logic and laws implemented in the real PLC of the test bench. These control laws were defined during the design phase of the multi-stacks testing equipment and aim to provide the desired conditions to the stacks, guaranteeing the safety of the installation and its components.

The control model has been developed using Simulink R2023b and the Stateflow library (The MathWorks Inc. 2025b). FMIKit v3.1 was used to to the plant's FMU integration instead of the native FMU integration block (Dassault Systèmes 2023). The FMU is cosimulated in Simulink and use its intern solver. Simulink model is simulated with a discrete fixed-step solver with a time-step of 1 s to be representative of real-PLC behavior. Communication time step between the FMU and the control model is inherited from Simulink solver (1 s).

These strategies have been tested on plant model presented in Section 2.2 in order to explore their limits before an implementation on the real system. The following section presents the simulation results obtained and a comparison with the corresponding experimental sequence.

#### 3 Results

#### 3.1 Initial conditions and results configuration

Before this study, the four stacks were operated in various conditions during several thousands of hours

and as the degradation phenomena has impacted them differently, the temperature corresponding to the thermoneutral voltage (for a given set of operating conditions j and SC) is not the same for each stack. Because there is no individual temperature control implemented in this system, it was chosen to control the hotbox temperature on the stacks' mean voltage.

To assess the response of the multi-stack testing equipment to the two transition strategies and to ensure a significant variation in  $H_2$  production (approximately 10%), the operating condition changes outlined in Table 1 were selected for the experiments. These conditions take into account the limits on the real system such as the pressure or the maximal temperature allowed in the stacks and the maximum SC value. Moreover, the system efficiency is not in the scope of this study and regarding the level of degradation at the time of the test, the conditions are representative of a real system operation.

**Table 1.** Operating points of the study, normalized by cell's active area for the current density and the fuel flow rate

	OP71	OP63	<i>OP67</i>
Current density $i$ [ $A.cm^{-2}$ ]	0.71	0.63	0.67
Steam Conversion <i>SC</i> [%]	55	55	55
Inlet fuel flow rate $[NmL.min^{-1}.cm^{-2}]$	10.05	8.88	9.43
$H_2O / H_2$ [%] mol. frac.	90 / 10	90 / 10	90 / 10

#### 3.2 Results description

The results shown in Figure 5 represent a succession of four transition sequences (two per strategy type). For each one, it starts from a nominal  $H_2$  production, goes to a lower one before going back to the nominal. Two fast transition sequences are represented between 0 and 6 hours with variations from OP71 to OP63 to OP67 to OP71. Two slow transition sequences are represented between 6 and 18 hours with variations from OP71 to OP63 to OP71. Each sequence is highlighted with gray vertical area.

The current density is proportional to the  $H_2$  production rate. In the transition from OP63 to OP71, a step at OP67 was needed because of pressure limitations on the system due to a high fuel flow rate value (low SC). All the changes on the parameters leading to a voltage evolution are done with the objective of maintaining the stacks' average voltage around the thermoneutral voltage, between 1.287 and 1.29 V (green area). The studied temperature is an average of fuel outlet temperature of the stacks. This average is displayed subtracting the initial temperature in

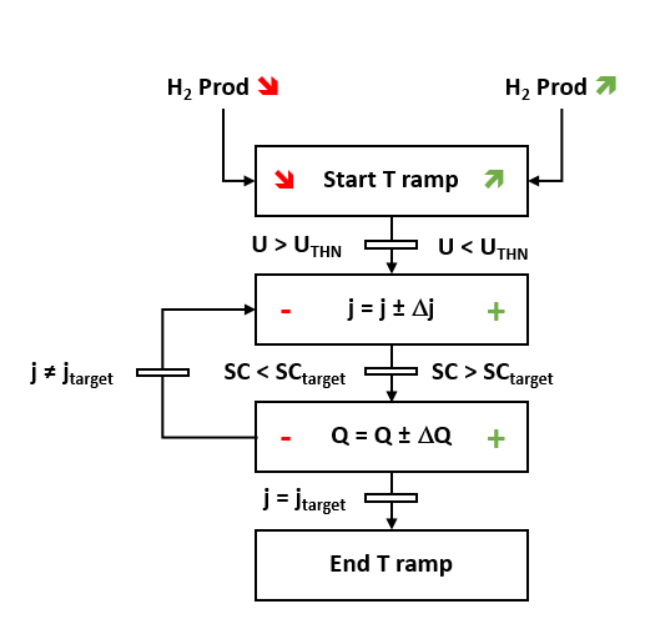


**Figure 3.** Slow operating point transition control state diagram

order to highlight the variation between the model and the real data, in which the absolute temperature initial values are different (degradation mechanisms are not all represented in the electrochemical model used). The fuel inlet flow rate is adjusted following the SC targeted at 55 %.

The described conditions have been reproduced in simulation (Figure 5). Computation time to simulate the sequences is about 10h20 with CPU 8th Gen Intel(R) Core(TM) i5-8365U 1.60 GHz and 16 Go RAM.

# 3.3 Comparison between experimental and model results

As a preliminary remark, it is important to mention that model is not fitted to real system. Main dynamics are represented by the model and it is used to test and debug control transitions. Model fitting using experimental data is a work in progress.

Overall, the model results are in accordance with the experimental data. One of the main difference between the model and real system is the thermal behavior. Even if the model describing the thermal phenomena occurring inside the hotbox, the stacks and between them is accurate comparing to 3D CFD simulations, some parameters are difficult to set precisely (as the thermal capacities for the conduction or the thermal emissivity of the materials for the radiation). It leads to differences, especially in term of dynamic behavior, which induce time shifts in the transitions, but also in term of absolute temperature value. However, it is worth noting that the main trends are

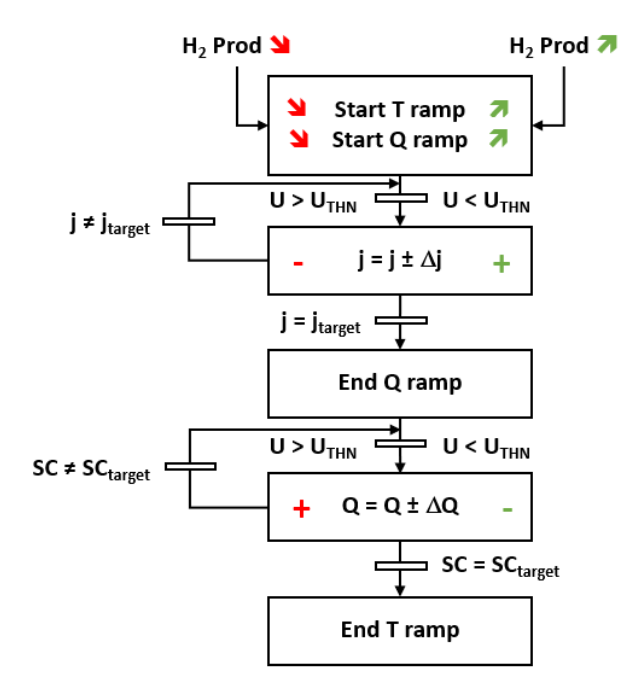


**Figure 4.** Fast operating point transition control state diagram

represented and the order of magnitude of the temperature difference between an operating point to another is consistent (about 10 °C for experimental data and about  $7 \, {}^{\circ}C$  for simulation). Inertia phenomena are observed on temperatures between sequences and the inverse trends are also observed in voltages, which is the expected behavior as proved by the experimental data. more, trends and variation orders are consistent between model and experimental data. Another main difference is observed on SC and fuel inlet flow rate during the second sequence (fast transition from OP63 to OP67). This important difference, about 3  $NmL.min^{-1}.cm^{-2}$ for flow rate and 10 % for SC, can be explained by the cyclic pressure variations occurring on the test bench steam generator during the re-filling with cold water. The fuel flow rate, hence the SC, is directly impacted. These variations are not represented in the model which can also explain some time shift observed during transition phases. As these flow rate variations are periodic, it could be interesting to reproduce them in the model.

Despite these differences between the model and the real system, the model allows to validated the control behavior for the proposed transition strategies by pointing out the limits of these strategies.

# 3.4 Results analysis and transition methods comparison

The objective of the slow strategy is to reach the new production point by maintaining the steam conversion while the temperature ramp is affecting the voltage. As the overall dynamic is led by the temperature, the flow

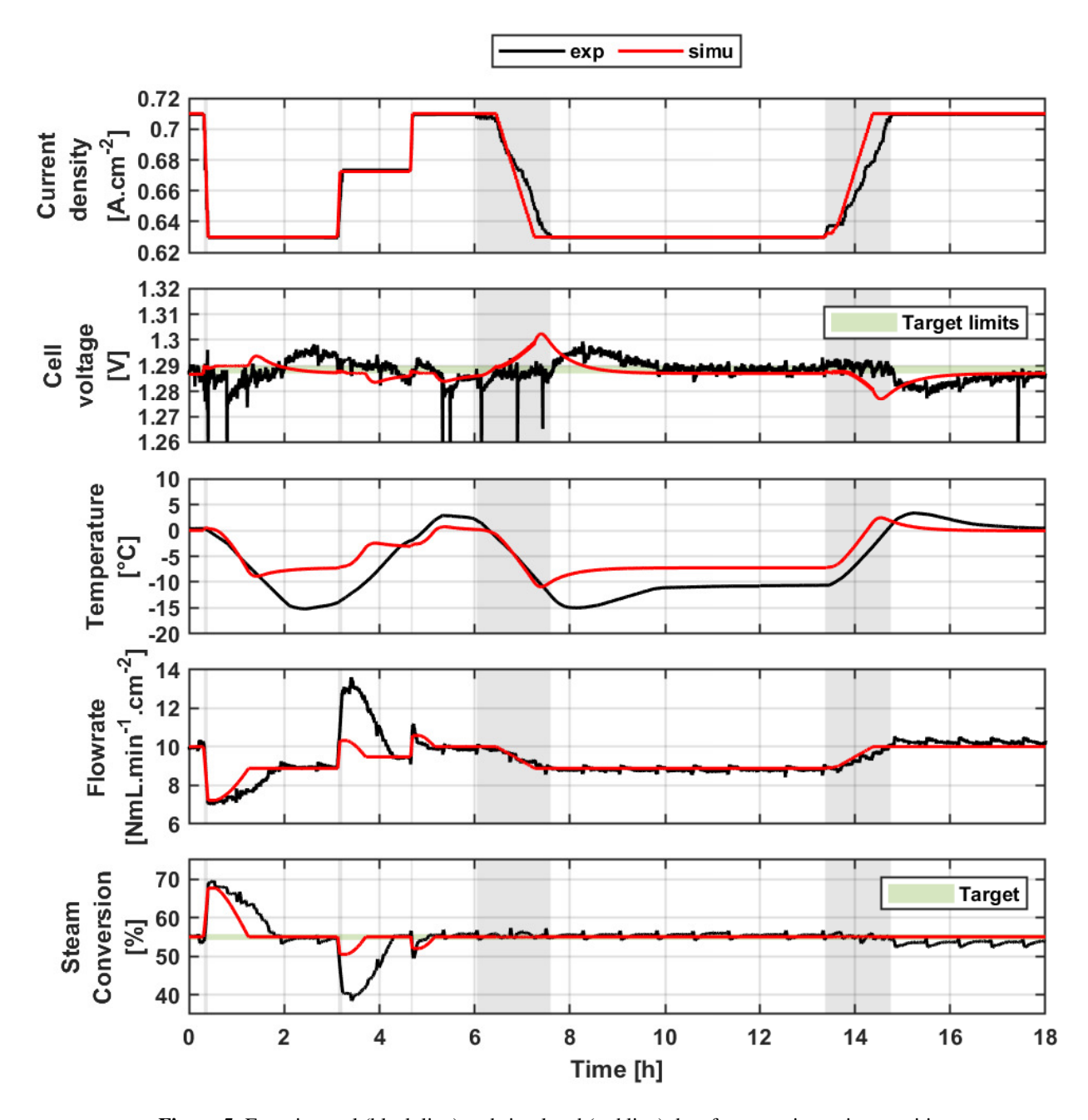


Figure 5. Experimental (black line) and simulated (red line) data for operating point transitions.

rate transition is smooth. It ensures safe conditions for the stacks.

The objective of the fast transition is to reach a new production point as soon as possible. To do so, and because the mean voltage is required to be maintained at its thermoneutral value, the only possible way is to allow variations on the flow rate (and so the SC).

The expected behavior for each strategy is clearly visible on the results. With the fast transition, the targeted production is reached ~20 time faster than with the slow one (5 minutes versus 1 hour 35 minutes).

In any case, both strategies led to a similar time for having the required operating point conditions (current density and SC). This is because the thermal dynamic is the slowest and therefore the one leading the system behavior.

To conclude this comparison, the advantages and drawbacks of each strategy can be sum-up in the following lists:

• Slow transition: The targeted production rate is reached slowly, but with a constant SC during the transition that limits the risks of having a critical value for the stacks (too high SC for less *H*<sub>2</sub> production and too high pressure due to a too low SC for more *H*<sub>2</sub> production).

• Fast transition: The targeted production rate is reached quickly. The SC is variable during the transition so the system limits need to be carefully characterized, and the safety actions adapted to avoid critical damages to the stacks.

The fast transition allows a faster way to accommodate the production rate of the system and can be of interest for some applications where the load profile is not fully stable or in a scenario with variable current input such as in some renewable energy sources. On the other side, it is less smooth than the slow transition and could be the source of accelerating stacks' degradation.

#### 4 Conclusions and discussions

This paper describes a Model in the Loop methodology to de-risk the implementation of new control strategies for a real SOEL system. A dynamic multi-physic model of the real system has been developed using Modelica language (supported by Dymola software). Then, this model has been exported as a FMU for being co-simulated in Simulink software where the control model was developed. This approach has been used to validate strategies of operating point transitions and corresponding results are discussed.

It is worth noting that this approach is sensitive to the level of implementation of the FMI standard of each software used. This is exemplified by its application to another SOEL system model, implemented in Modelica using another proprietary library and comprising more components. Even though the plant model run with its own control without errors in Dymola, trying to implement the same control in Simulink and applying it to the corresponding FMU of the Modelica plant model resulted in difficulties during simulation (extreme slowness and generally ending up with errors). Those difficulties have been observed and the identification of bottlenecks is non-trivial task. Future studies focused on model stability are considered.

Future objective for this model is Hardware in the Loop and/or Control Hardware in the Loop approach. Thus, many challenges can be addressed on the model such as fitting, adaptation and simplification to be compatible for real-time computer with a consistent representativeness. Concerning the control model, specific toolbox enabling a transfer of control developed in Simulink to real PLC can be tested. Moreover, in the present work, robust control has not been explored considering uncertainties in the model parameters. This aspect could be investigated to improve performance under such uncertainties.

### **Acknowledgements**

The authors gratefully acknowledge the financial support by CEA, GENVIA and partially by the REVERSI ADEME project.

#### References

- Andersson, Daniel et al. (2011-03-20). "Dynamic modeling of a solid oxide fuel cell system in Modelica". In: *Proceedings 8th Modelica Conference*. Dresden, Germany, pp. 593–602. DOI: http://dx.doi.org/10.3384/ecp11063.
- Aoun, Nadine et al. (2019-02). "Dynamic Simulation of Residential Buildings Supporting the Development of Flexible Control in District Heating Systems". In: Proceedings of the 13th International Modelica Conference, Regensburg, Germany, March 4–6, 2019. Vol. 157. Linköing University Electronic Press, pp. 129–138. DOI: 10.3384/ecp19157129.
- Botta, G. et al. (2019). "Dynamic modeling of reversible solid oxide cell stack and control strategy development". In: *Energy Conversion and Management* 185, pp. 636–653. ISSN: 0196-8904. DOI: https://doi.org/10.1016/j.enconman.2019. 01.082. URL: https://www.sciencedirect.com/science/article/pii/S0196890419301360.
- Cech, Martin et al. (2017). "Novel tools for model-based control system design based on FMI/FMU standard with application in energetics". In: pp. 416–421. DOI: 10.1109/PC. 2017.7976250.
- Cubizolles, Géraud et al. (2024-10). "Development of a Versatile and Reversible Multi-Stack Solid Oxide Cell System Towards Operation Strategies Optimization". In: *Journal of The Electrochemical Society* 171.10, pp. 104–511. DOI: 10.1149/1945-7111/ad85fa.
- Dassault Systèmes (2023). *FMIKit-Simulink*. URL: https://github.com/CATIA-Systems/FMIKit-Simulink.
- Dassault Systèmes (2025). *Dymola*. URL: https://www.3ds.com/products/catia/dymola.
- Ensbury, Theodor, Nate Horn, and Mike Dempsey (2020). "Dymola and Simulink in Co-Simulation: A Vehicle Electronic Stability Control case study". In: American Modelica Conference 2020. URL: https://www.claytex.com/wp-content/uploads/2021/06/Dymola-and-Simulink-in-Co-Simulation\_-a-case-study.pdf.
- Iyer, Siddharth et al. (2024-06). "Review of experimental and modelling investigations for solid oxide electrolysis technology". In: *International Journal of Hydrogen Energy* 72, pp. 537–558. DOI: 10.1016/j.ijhydene.2024.05.312.
- Laurencin, J. et al. (2011). "Modelling of solid oxide steam electrolyser: Impact of the operating conditions on hydrogen production". In: *Journal of Power Sources* 196.4, pp. 2080–2093. DOI: 10.1016/j.jpowsour.2010.09.054.
- Modelica Association (2014). Functional Mock-up Interface for Model Exchange and Co-Simulation version 2.0. Tech. rep. Modelica Association. URL: https://fmi-standard.org.
- Modelon AB (2021a). Fuel Cell Library Version 1.13. Tech. rep. Modelon AB. URL: https://modelon.com/library/fuel-cell-library/.
- Modelon AB (2021b). *Modelon Base Library Version 3.7*. Tech. rep. Modelon AB. URL: https://modelon.com/modelon-library-suite-modelica-libraries/.
- Pohjoranta, Antti et al. (2015-03). "Model predictive control of the solid oxide fuel cell stack temperature with models based

- on experimental data". In: *Journal of Power Sources* 277, pp. 239–250. DOI: 10.1016/j.jpowsour.2014.11.126.
- The MathWorks Inc. (2025a). *MATLAB/Simulink*. URL: https://mathworks.com/products/simulink.html.
- The MathWorks Inc. (2025b). *Stateflow*. URL: https://fr.mathworks.com/products/stateflow.html.
- Wang, Kai et al. (2017). "Integration of complex Modelica-based physics models and discrete-time control systems: Approaches and observations of numerical performance". In: 12th International Modelica Conference, Prague, Czech Republic, May 15-17, 2017, pp. 527–532. DOI: 10.3384/ecp17132527.
- Zimmer, Dirk (2019-02). "Towards Hard Real-Time Simulation of Complex Fluid Networks". In: *Proceedings of the 13th International Modelica Conference, Regensburg, Germany, March 4–6, 2019.* Vol. 157. Linköing University Electronic Press, pp. 579–588. DOI: 10.3384/ecp19157579.